JASA Express Letters

NOVEMBER 21 2023

Sound power of NASA's lunar rocket System versus Saturn V

Makayle S. Kellison; Kent L. Gee

Check for updates

JASA Express Lett. 3, 113601 (2023)
https://doi.org/10.1121/10.0022538

JASA EXPRESS LETTERS ARTICLE asa.scitation.org/journal/jel

Sound power of NASA's lunar rockets: Space Launch System versus Saturn V

Makayle S. Kellison[1] **and Kent L. Gee**[2,a)]
[1]*Department of Physics, Rollins College, Winter Park, Florida 32789, USA*
[2]*Department of Physics and Astronomy, Brigham Young University, Provo, Utah 84602, USA*
mkellison@rollins.edu, kentgee@byu.edu

Abstract: To improve acoustical models of super heavy-lift launch vehicles, this Letter reports Space Launch System's (SLS's) overall sound power level (OAPWL) and compares it to NASA's past lunar rocket, the Saturn V. Measurements made 1.4–1.8 km from the launchpad indicate that SLS produced an OAPWL of 202.4 (±0.5) dB re 1 pW and acoustic efficiency of about 0.33%. Adjustment of a static-fire sound power spectrum for launch conditions implies Saturn V was at least 2 dB louder than SLS with approximately twice the acoustic efficiency.

[Editor: Siu-Kit Lau] https://doi.org/10.1121/10.0022538

Received: 11 October 2023 **Accepted:** 7 November 2023 **Published Online:** 21 November 2023

1. Introduction

Nearly 50 years after the Saturn V's final flight, NASA's Space Launch System (SLS) launched the Artemis-I mission as part of a broader program (Smith *et al.*, 2020; Creech *et al.*, 2022) to return humans to the moon and beyond. As this launch commenced a new era of lunar space travel, an acoustical measurement campaign was performed to understand the noise produced by super heavy-lift vehicles. Initial analyses of sound levels measured during the Artemis-I mission are described by Gee *et al.* (2023) and Kellison *et al.* (2023). This Letter furthers these results by reporting a sound power analysis of SLS and comparing NASA's current lunar rocket to the Saturn V.

At present, these super heavy-lift launch vehicles represent the most powerful rockets lifted into orbit. Rapid progression of rocket development and an increased global launch cadence motivate a greater need to understand the physics of these complex systems. Investigation into the sound produced by launch vehicles began in the late 1950s with the first Space Age (Cole *et al.*, 1957; Mayes *et al.*, 1959; Mayes and Edge, 1962; Wilhold *et al.*, 1963; Potter and Crocker, 1966; Guest and Jones, 1967), and much of this work culminated in the source models found in NASA SP-8072 (Eldred, 1971). Yet, known limitations with SP-8072 and related models, as well as differences between modern and historical launch vehicles, necessitate revisions to these approaches (Lubert *et al.*, 2022).

Updated models rely, in part, on improved rocket noise measurements and corresponding analyses (Kenny *et al.*, 2009; Fukuda *et al.*, 2009; James *et al.*, 2014; Mathews *et al.*, 2021; Hart *et al.*, 2022). Of particular interest is the vehicle's sound power, which is used as the foundation for source radiation models. Although each vehicle's sound power differs because of nozzle size, thrust, and other plume parameters, acoustic efficiency, η, is used to compare sound power across launch vehicles and other jets. Eldred (1971) compiled values for η, defined as the ratio of the vehicle's acoustic power to its mechanical power, from several studies. Most values—many of them from rockets much smaller than those typically launched today—ranged from 0.1% to 1.0%, representing a 10 dB spread in overall sound power level (OAPWL) for a given mechanical power.

Despite this considerable data scatter, Mayes *et al.* (1959) suggested the acoustic efficiency for rockets to be 0.5%, a value that has been used in other studies (e.g.,Varnier, 2001; Kumar and Karthikeyan, 2013; Morshed *et al.*, 2013; Gee *et al.*, 2022). Relatively recent measurements of solid-fuel rockets have reported 0.4%–0.8% (Campos, 2005; Fukuda *et al.*, 2009; James *et al.*, 2014; Lubert *et al.*, 2022) for η, whereas sound power estimates from recent orbital launches have suggested ∼0.3% (Mathews *et al.*, 2021; Hart *et al.*, 2022). Yet, significant gaps in calculation methodologies still exist, including rigorous consideration of ground reflections in many studies (Hart and Gee, 2023).

To document the OAPWL and η of NASA's current super heavy-lift launch vehicle, this Letter reports measurements from the SLS Artemis-I mission. The OAPWL and η are presented from four stations around the launchpad at a distance of ∼1.4–1.8 km. Additionally, one-third octave (OTO) band sound power spectra are analyzed at the four locations, and an averaged octave-band spectrum is compared to that of the Saturn V.

[a)]Author to whom correspondence should be addressed.

2. Launch and measurement description

The SLS Artemis-I mission lifted off on 16 November 2022 from Launch Complex 39B (LC-39B) at Kennedy Space Center (KSC). Far-field acoustical measurements were made at ten autonomous stations located within KSC and seven manned stations off-Center. While initial analyses have been performed for several stations both on- (Gee *et al.*, 2023) and off-Center (Kellison *et al.*, 2023), this Letter focuses on four stations located ∼1.4–1.8 km from LC-39B. These stations, labeled P05, P06, P07, and P09, and their corresponding distances from the pad are displayed in Fig. 1(a). Within road access constraints, the measurement stations were strategically placed in rough cardinal directions around LC-39B to capture any azimuthal (ϕ) source directionality.

Each measurement station consisted of a portable unit for measuring acoustics (PUMA), which was comprised of a weatherproof case with a ruggedized computer, a Global Positioning System (GPS) time clock for synchronization, NI 9250 24-bit/5-V and NI 9232 24-bit/30-V data acquisition modules sampling at 102.4 kHz, and a lithium-ion battery (Gee *et al.*, 2020). At these stations, GRAS 6.35 mm (1/4 in.) 46BE condenser, free-field microphones (4 Hz – 80 kHz) were used (GRAS, 2023). Although free-field microphones are designed for normal incidence, the response difference for other angles is insignificant out to the maximum analysis frequency of 10 kHz. However, because rocket noise often includes significant energy below 4 Hz, the microphones' low-frequency response was adjusted using digital filtering to extend below 1 Hz (Marston, 2008; Rasband *et al.*, 2023). The microphones were set up inverted above a plastic 40.6 cm (16 in.) diameter ground plate under a porous foam windscreen with a 3.8 cm (1.5 in.) uniform thickness. This configuration (Anderson *et al.*, 2022), nicknamed the compact outdoor unit for ground-based acoustical recordings (COUGAR), is observed in Figs. 1(b) and 1(c). Multiple rocket launch, sonic boom, and jet noise measurement campaigns have successfully used PUMAs and COUGARs to collect acoustic data.

During the Artemis-I mission, a combined 39.1 MN of thrust launched SLS, making it the most powerful rocket to successfully reach orbit. Its core stage, powered by four Aerojet Rocketdyne (El Segundo, CA) RS-25 liquid hydrogen-oxygen engines, is flanked by two Northrop Grumman (Corinne, UT) five-segment solid-fuel rocket boosters (SRBs). The

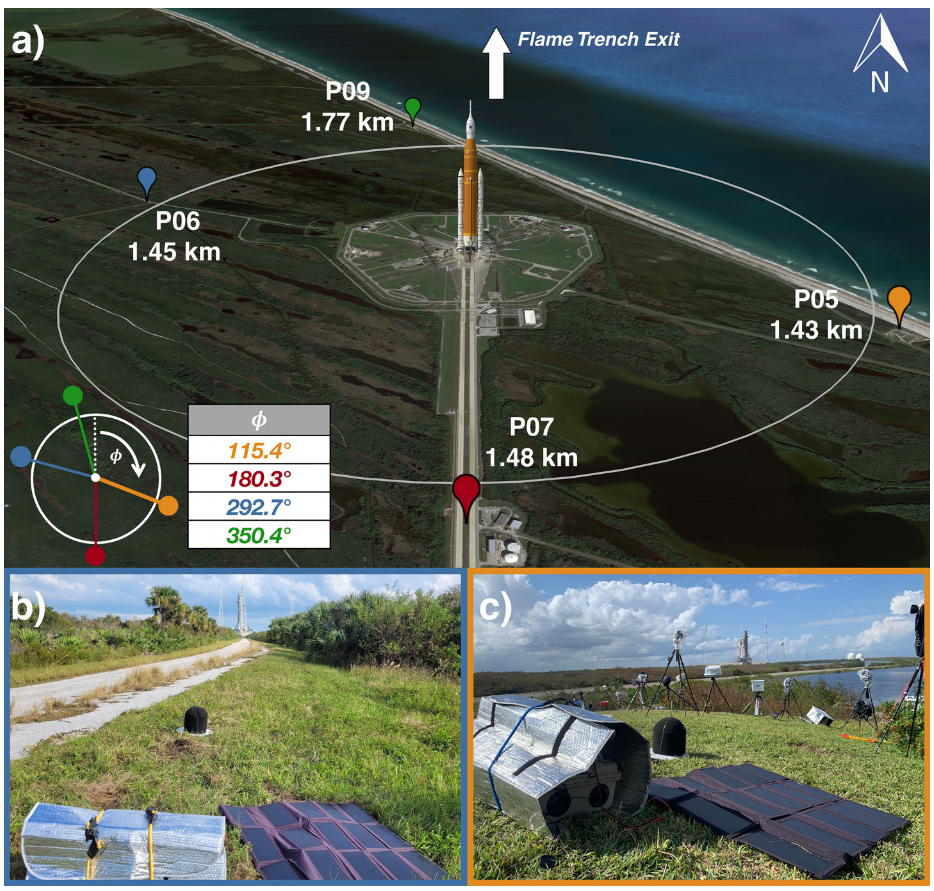

Fig. 1. (a) Four autonomous measurement stations on-Center annotated with their distances and azimuths (ϕ) from LC-39B. A white circle represents the blast danger area, and a SLS model (not to scale) is included. Measurement stations P06 (b) and P05 (c) are pictured relative to their views of the launchpad.

SRBs provide ~82% of the total thrust and, therefore, dominate the rocket's noise radiation. Note that the relative separation and orientation of SLS's nozzles, as well as the use of SRBs, distinguishes this launch vehicle from the Saturn V. With a thrust of 34.8 MN, Saturn V used five Rocketdyne F-1 liquid engines clustered such that early plume merging and azimuthal symmetry could be assumed (Eldred, 1971).

Because of the possibility for azimuthal variability impacting sound power calculations, SLS's orientation on the pad and after liftoff is pertinent to the discussion in this Letter. Before vehicle liftoff, P07 (south) and P09 (north) viewed the core stage and both SRBs. In contrast, P05 and P06, located more east and west [see Fig. 1(a)], predominantly saw a single SRB. As it lifted off, the vehicle remained in this orientation until $T+8$ s, when its roll maneuver began. Mm. 1 shows liftoff from two different camera views and highlights the 90° roll from $T+8$ s to $T+18$ s, as well as the expanding vapor cloud to the north of the flame trench. After the roll was completed, P07 and P09 viewed the vehicle's side (single SRB) while P05 and P06 essentially viewed the entire core stage and both SRBs. Around $T+20$ s, the vehicle began to pitch over along its easterly trajectory.

Mm. 1. Time-synchronized videos showing two views of the SLS Artemis-I liftoff. Original footage is available online (NASA, 2022a,b).

3. Sound power calculation

The vehicle's trajectory is used with measured acoustic data to calculate SLS's radiated sound power and determine η. After outlining the methods used to obtain these results, OAPWL and η are calculated for all four stations. Additionally, a power spectral analysis allows for comparisons between SLS and the Saturn V in Sec. 4.

3.1 Method overview

A typical calculation of sound power is based on a stationary source and a collection of microphones that map the sound field around it (e.g., ISO, 2003; Fritze *et al.*, 2009). However, with a launched rocket and present measurement capabilities, the source moves relative to a single, stationary microphone. Therefore, different methods to calculate sound power are required. The procedure, used previously by Mathews *et al.* (2021) and Hart *et al.* (2022), determines the time-varying position and rocket orientation in relation to the microphone. Although sound radiation may vary with polar and azimuthal angles, azimuthal symmetry is assumed in obtaining OAPWL. The calculation ultimately requires knowledge of two trajectory-related variables: r, the distance between the base of the moving vehicle and the stationary microphone, and θ, the polar angle between the plume and the microphone. Although the noise is generated downstream of the nozzle exit, the microphones are sufficiently in the far field that the vehicle base is a suitable origin. The angle is defined relative to the plume exhaust direction, such that $\theta \approx 90°$ for a ground-based microphone as the vehicle lifts off the pad. Note that although plume impingement alters the sound source during liftoff, the plume can be considered undeflected because of the microphones' far-field location and the emission angles dominating sound power.

Finding the rocket's sound power begins with a shift of trajectory time base from emission time to observer time. Measured acoustic data are inherently in observer time due to sound propagation, but trajectory data are in emission time. To tie sound levels to trajectory data, these time bases must be connected through a propagation delay of r/c, where the sound speed, c, is assumed to be 344 m/s based on the ambient conditions. With trajectory and microphone data in observer time, running overall sound pressure levels (OASPLs) and frequency-dependent sound pressure levels are distance-corrected using spherical spreading to a common reference of 1.43 km, which is the distance to P05. The next step in calculating sound power is to express θ in observer time, using Eq. (1) in Hart *et al.* (2022). Distance-corrected pressure levels are then expressed as a function of θ using the common variable of observer time, effectively creating a directivity function at 1.43 km. Finally, the angle-dependent mean-square pressures are integrated to obtain sound power using the equations outlined in Leishman *et al.* (2006) and simplified for the axisymmetric radiation case by Matoza *et al.* (2013), who used static rocket data to justify disregarding $\theta > 90°$ in OAPWL calculations by showing that these angles contribute negligibly to the total radiated power. Once the OAPWL is found, 3 dB is subtracted to account for a COUGAR microphone near a finite-impedance ground surface (Hart and Gee, 2023). Note that this sound power calculation procedure can be applied to OASPL to obtain OAPWL or to frequency-dependent pressure levels to obtain sound power level (PWL) spectra.

3.2 OASPLs

Because distance-corrected OASPLs are used in calculating SLS's OAPWL, examining the pressure levels as a function of time and θ helps justify the azimuthal symmetry assumption in the power methodology. Whereas distance-corrected levels can be expressed in either observer or emission time, displaying them as a function of emission time allows for levels to be examined for time-dependent azimuthal variation. Distance-corrected OASPL at all four stations is shown as a function of emission time in Fig. 2(a) and as a function of θ in Fig. 2(b). There are two noteworthy observations from Fig. 2(a). First, the flame trench causes highly directional noise radiation until $T+5$ s as P09's levels are ~15 dB greater than those for P07 (in the opposite direction). Although this comparison is important for understanding launchpad effects on sound radiation, the range of θ spanned in Fig. 2(b) during the first several seconds of launch is small such that it does not impact the OAPWL calculation. Consequently, early-launch azimuthal asymmetry is not addressed further in this Letter.

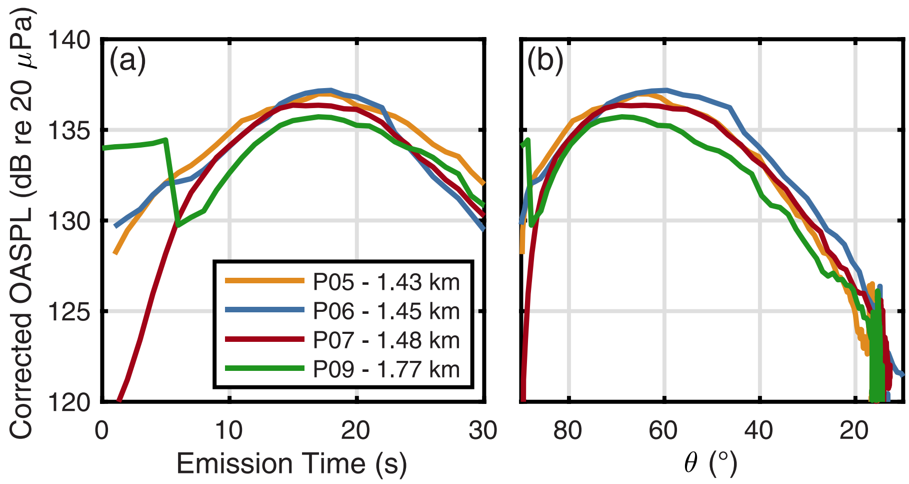

Fig. 2. Artemis-I OASPLs at four measurement stations, which are distance-corrected to 1.43 km as a function of (a) emission time and (b) polar angle, θ.

Second, the maximum OASPL at all four stations occurs during the $T+8$ s–$T+18$ s roll maneuver, complicating efforts to understand effects of nozzle configuration on noise radiation. However, because OASPL differences across the stations span only ± 1 dB beginning at $T+6$ s, assumed azimuthal symmetry in power calculations appears justified. As a result, the vehicle's OAPWL is obtained by averaging the power level calculated at each station.

Although a detailed directivity analysis is reserved for future work, a brief examination of the corrected OASPL(θ) in Fig. 2(b) helps establish data validity. Across the locations, the maximum directivity angle for SLS noise radiation during liftoff ranges from 60° to 70° with an angular lobewidth (–3 dB) of ~40°. These observations align with findings from other rockets. First, similar solid rocket boosters (SRBs), including the Space Shuttle's RSRM (Lubert *et al.*, 2022) and the Atlas V's GEM-63 (Bassett *et al.*, 2021), have maximum directivity angles of 60°–65°. Second, SLS's lobewidth is consistent with the 30°–40° lobewidth for various static firings (Cole *et al.*, 1957; Eldred, 1971; Kenny *et al.*, 2009; Fukuda *et al.*, 2009) and launched vehicles (Mathews *et al.*, 2021; Hart *et al.*, 2022). Because of their importance in power calculations, this agreement of the peak directivity angle and lobewidth with other rocket measurements provides a degree of confidence in the reported OAPWL values.

3.3 OAPWLs

Table 1 displays SLS's OAPWL for all four stations along with their corresponding distances from LC-39B. Although representing independent measurements and calculations, all values fall within a 1 dB range, resulting in a (decibel) average OAPWL of 202.4 dB re 1 pW. (The 1 pW power reference is assumed hereafter.) For context, the OAPWL of an afterburning T-7A aircraft is 173 dB (Christian *et al.*, 2023), meaning nearly 900 T-7As are required to match SLS's sound power during launch.

In addition to OAPWL, Table 1 also shows the calculated η for each station. For SLS, η ranges from 0.29%–0.37% with an average of 0.33%. Translated into decibels, the difference between a historically assumed 0.5% and a measured 0.33% for SLS is 1.8 dB. This is not the first modern launch measurement to suggest an efficiency lower than 0.5%. Recent measurements of the Delta IV Heavy (Hart *et al.*, 2022), with its triple-body configuration somewhat similar to SLS, yielded an η of 0.3%. Although this efficiency is similar to $\eta \approx 0.33\%$, the Delta IV Heavy study did not account for ground reflections, meaning that $\eta < 0.3\%$ in actuality—even farther from 0.5%. Given the historical literature's ambiguity regarding the treatment of ground reflections in OAPWL calculations, there is an ongoing need to improve understanding of η for different rockets and launch scenarios.

Table 1. SLS's OAPWL and acoustic efficiency at four measurement stations.

Station	Pad distance (km)	OAPWL (dB re 1 pW)	η (%)
P05	1.43	202.6	0.34
P06	1.45	202.9	0.37
P07	1.48	202.2	0.31
P09	1.77	201.9	0.29
Average	1.53	202.4	0.33

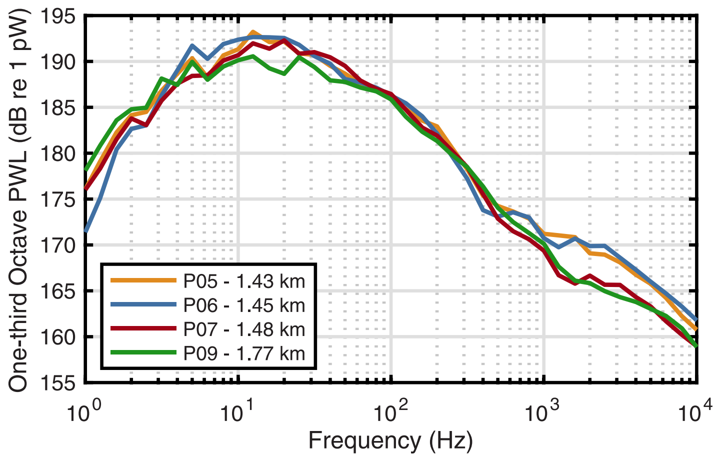

Fig. 3. OTO band PWL spectra for P05, P06, P07, and P09 located in approximate cardinal directions relative to the launchpad.

3.4 Sound power spectra

The sound power methodology used to obtain OAPWL is applied to each frequency band individually to calculate sound power level spectra, PWL(f). Figure 3 shows OTO-band PWL(f) for all four stations with strong similarities among spectral curves. In the lowest-frequency region (<10 Hz), the data spread across stations is ∼2–3 dB with relatively random scatter. Additionally, all stations have a peak frequency value of ∼10–20 Hz, which is similar to the maximum sound pressure level spectra (Gee *et al.*, 2023). Between about 50 and 500 Hz, the PWL(f) from all four stations collapses remarkably well. It is above 500 Hz that the high-frequency behavior at each station differs most significantly in a seemingly nonrandom way. Stations P05 and P06 have greater high-frequency content (∼5 dB) than P07 and P09. Because this is the only major distinguishing factor when comparing the north and south stations (P09 and P07) and the east and west stations (P05 and P06), future investigations will determine if this spectral difference is evidence of frequency-dependent azimuthal asymmetry.

4. SLS versus Saturn V: A sound power comparison

With the launch of SLS came many inquiries about its comparison to NASA's past lunar rocket, the Saturn V. This section seeks to answer the question: which of NASA's super heavy-lift launch vehicles—SLS or Saturn V—is louder? Although measured sound power does not correlate perfectly with loudness, the vehicles' spectral similarities allow this question to be answered with reasonable certainty.

Although acoustical measurements of equal fidelity were not made during the Apollo missions, past work (Gee *et al.*, 2022) suggested that the Saturn V's OAPWL was ∼203–204 dB. Because this estimate is greater than SLS's OAPWL, it is worth scrutinizing these results more carefully to determine the validity of this initial comparison. Thus, precision to the tenth of a decibel is used in the below calculations before making final approximations that acknowledge uncertainties in historical data.

The Saturn V's estimated OAPWL was based on an assumed $\eta = 0.5\%$ and two reports (Kramer, 1966; Allgood, 2012) of first-stage vertical static tests at NASA Stennis Space Center. In particular, the report by Kramer (1966) shows a free-space PWL(f), which is reproduced in Fig. 4. The corresponding OAPWL for a static-fired Saturn V is 202.7 dB with $\eta = 0.41\%$, which is somewhat larger (∼1 dB) than the acoustic efficiency of SLS at 0.33%. Figure 4 compares Kramer's sound power spectrum with SLS's spectrum, which was produced by averaging the spectra in Fig. 3 and then integrating into octave bands. Inspection of these curves reveals their similar shapes and nearly identical peak frequencies.

From Fig. 4, it could be concluded that SLS and Saturn V produced nearly identical sound power spectra and were, therefore, equally loud. However, one key difference between these curves remains: the SLS sound power spectrum was for a launched vehicle and the Saturn V PWL(f) was calculated from a vertical static firing with a plume deflector. Correcting the 202.7 dB static-fire estimate to account for an undeflected plume produces a more accurate representation of a launched Saturn V's sound power and corresponding acoustic efficiency. Based on the work of Cole *et al.* (1960), Eldred (1971) discussed the variation in η for different-shaped plume deflectors, all of which reduced OAPWL and efficiency relative to an undeflected plume. From Fig. 4 in Eldred (1971), the two deflectors studied were a curved 45°-deflection plate (–5.2 dB) and a 150°-deflection closed-bucket deflector (–1.2 dB). Because its curved, open deflector redirected the plume by more than 90°, the Stennis deflector falls between these two cases. Based on the composite results, a 2.0 dB increase in OAPWL is assumed here for a launched Saturn V with undeflected plume relative to the static firing. Although somewhat arbitrary, this estimated increase is also likely conservative, especially given that the static test facility

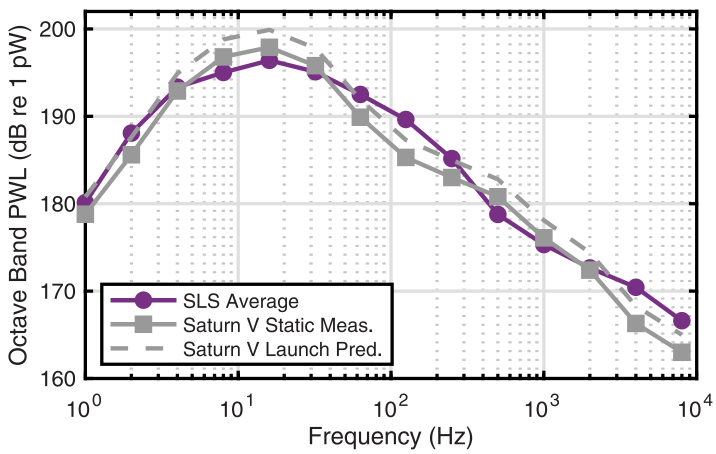

Fig. 4. Measured octave-band PWL(f) for SLS along with a Saturn V vertical static firing (Kramer, 1966). The dashed line represents the predicted spectrum for a launched Saturn V by assuming a uniform 2 dB increase over the static firing levels.

included a water deluge system that would have reduced η further (Kramer, 1966). This simple model predicts the launched Saturn V to have an OAPWL of 204.7 dB as depicted in the last row of Table 2 and the dashed line in Fig. 4. When compared to SLS's 202.4 dB OAPWL, the launched Saturn V would be at least 2.3 dB louder than SLS.

It is also worthwhile to consider the vehicles' radiation efficiencies. Assuming the same η, Saturn V should radiate less sound power (–0.7 dB) than SLS. For $\eta = 0.33\%$, the OAPWL of a launched Saturn V would be 201.7 dB. Instead, the launch-adjusted prediction of 204.7 dB is 3 dB greater, corresponding with a factor of 2 increase in η. Therefore, $\eta \approx 0.66\%$ for a launched Saturn V, which is based on the data in Kramer (1966) and the adjustment here. Note that this predicted η and OAPWL (see Table 2) increases estimates by Gee *et al.* (2022) for the Saturn V's power level by about 1 dB.

Differences in η and OAPWL might be explained by the two vehicles' nozzle configurations. Whereas the Saturn V's nozzle size and spacing likely produced rapid plume coalescence, SLS's SRB plumes remain well separated relatively far downstream (see Mm. 1). With a nozzle configuration somewhat similar to that of SLS, the Space Shuttle's PWL(f) was lower than predicted by several decibels (McInerny, 1992). However, the same modeling approach more accurately predicted Saturn V sound levels. McInerny suggested that Space Shuttle's η was reduced by the launch vehicle's asymmetry and shielding effects from the separated plumes.

As further evidence for Saturn V's greater source levels, sound pressure measurements are compared to Artemis-I data. Using Apollo-8 octave-band spectra (McInerny, 1992), Gee *et al.* (2022) showed OASPLs of 163.5, 155.3, and 152.0 dB re 20 μPa from three different measurement stations located 81.5, 183, and 366 m from the launchpad, respectively. Assuming spherical spreading, the Saturn V OASPLs at these three locations were extrapolated to the four SLS measurement distances. The 12 combinations of levels and distances, when compared to SLS OASPLs, indicate that the Saturn V levels were on average 1.5 dB greater, where 10 of the 12 differences were positive. This comparison strengthens the assertion that Saturn V's η and OAPWL were larger than those of SLS.

5. Conclusion

This Letter has documented the sound power of NASA's Space Launch System. Using far-field measurements ($\sim$1.4–1.8 km), the vehicle's average OAPWL is 202.4 ($\pm$0.5) dB re 1 pW with an acoustic efficiency of $\eta \approx 0.33\%$. The lack of variation in OAPWL, as observed from different directions, suggests little evidence of azimuthal asymmetry in overall sound radiation despite the vehicle's asymmetric nozzle configuration and separated plumes. However, differences in the one-third octave sound power spectra above 1 kHz possibly indicate frequency-dependent radiation asymmetries.

A comparison of NASA's lunar launch vehicles showed that Saturn V was louder than SLS as quantified by PWLs and spectra. After adjusting for plausible increases in acoustic efficiency to account for an undeflected plume

Table 2. Sound power and acoustic efficiency comparisons of SLS and Saturn V.

	OAPWL (dB re 1 pW)	η (%)
SLS average	202.4	0.33
Saturn V—Deflected plume	202.7	0.41
Saturn V—Undeflected plume (predicted)	204.7	0.66

(far-field launch conditions), Saturn V's OAPWL was likely ~2 dB greater than that of SLS with an acoustic efficiency approximately twice as large. As confirmation, Saturn V pressure levels were 1.5 dB greater when extrapolated to SLS's measurement locations, possibly implying that SLS's nozzle configuration caused a lower acoustic efficiency.

This potential explanation for the efficiency difference has implications beyond SLS and the Saturn V. If rockets with clustered, symmetric nozzle configurations (Saturn V) radiate more noise than vehicles with separated, asymmetric configurations (SLS), this has an immediate impact on vehicle vibroacoustic modeling and a potential long-term impact on vehicle design. Consequently, further investigation into the effects of different nozzle configurations on noise radiation is needed. This should include rockets with tightly clustered nozzles, such as SpaceX's Starship, to fully determine the acoustical impacts of next-generation super heavy-lift launch vehicles.

Acknowledgments

M.S.K. was supported in part by National Science Foundation (NSF) Research Experiences for Undergraduates (REU) Grant No. 2051129 and NSF Grant No. 2109932. The authors gratefully thank Mark C. Anderson for assistance with analysis and plot preparation. Logan T. Mathews is thanked for assisting with Mm. 1. Mark C. Anderson, Logan T. Mathews, Whitney L. Coyle, and Carson F. Cunningham are thanked for reviewing the manuscript.

Author Declarations

Conflict of Interest

The authors have no conflicts to disclose.

Data Availability

Some data that support the findings of this study may be available upon request from the corresponding author. The data are not publicly available due to security restrictions.

References

Allgood, D. C. (**2012**). "A brief historical survey of rocket testing induced acoustic environments at NASA SSC," Engineering Analysis Record 00294, NASA Document 20120003777, available at https://ntrs.nasa.gov/citations/20120003777 (Last viewed 14 November 2023).

Anderson, M. C., Gee, K. L., Novakovich, D. J., Mathews, L. T., and Jones, Z. T. (**2022**). "Comparing two weather robust microphone configurations for outdoor measurements," Proc. Mtgs. Acoust. **42**, 040005.

Bassett, M. S., Gee, K. L., Hart, G. W., Mathews, L. T., Rasband, R. D., and Novakovich, D. J. (**2021**). "Peak directivity analysis of far-field acoustical measurements during three GEM 63 static firings," Proc. Mtgs. Acoust. **39**, 040004.

Campos, E. (**2005**). "Prediction of noise from rocket engines," in *11th AIAA/CEAS Aeroacoustics Conference (26th AIAA Aeroacoustics Conference)*, 23–25 May, Monterey, CA (American Institute of Aeronautics and Astronautics, Reston, VA), AIAA Paper 2005-2837.

Christian, M. A., Gee, K. L., Streeter, J. B., Wall, A. T., and Campbell, S. C. (**2023**). "Sound power and acoustic efficiency of an installed GE F404 jet engine," JASA Express Lett. **3**, 073601.

Cole, J. N., England, R. T., and Powell, R. G. (**1960**). "Effects of various exhaust blast deflectors on the acoustic noise characteristics of 1,000 pound-thrust rockets," Wright Air Development Division Air Research and Development Command Technical Report 60-6 (Wright-Patterson Air Force Base, OH).

Cole, J. N., Von Gierke, H. E., Kyrazis, D. T., Eldred, K. M., and Humphrey, A. J. (**1957**). "Noise radiation from fourteen types of rockets in the 1,000 to 130,000 pounds thrust range," Wright Air Development Center Technical Report 57-354, AD 130794 (Wright Air Development Center, OH).

Creech, S., Guidi, J., and Elburn, D. (**2022**). "Artemis: An overview of NASA's activities to return humans to the moon," in *2022 IEEE Aerospace Conference*, March 5–12, Big Sky, MT (Institute of Electrical and Electronics Engineers, Piscataway, NJ), pp. 1–7, available at https://ntrs.nasa.gov/citations/20210026673 (Last viewed 14 November 2023).

Eldred, K. M. (**1971**). "Acoustic loads generated by the propulsion system," NASA SP-8072, available at https://ntrs.nasa.gov/citations/19710023719 (Last viewed 14 November 2023).

Fritze, D., Marburg, S., and Hardtke, H. J. (**2009**). "Estimation of radiated sound power: A case study on common approximation methods," Acta Acust. Acust.**95**, 833–842.

Fukuda, K., Fujii, K., Ui, K., Ishii, T., Oinuma, H., Kazawa, J., and Minesugi, K. (**2009**). "Acoustic measurements and prediction of solid rockets in static firing tests," in *15th AIAA/CEAS Aeroacoustics Conference (30th AIAA Aeroacoustics Conference)*, 11–13 May, Miami, FL (American Institute of Aeronautics and Astronautics, Reston, VA), AIAA Paper 2009-3368.

Gee, K. L., Hart, G. W., Cunningham, C. F., Anderson, M. C., Bassett, M. S., Mathews, L. T., Durrant, J. T., Moats, L. T., Coyle, W. L., Kellison, M. S., and Kuffskie, M. (**2023**). "Space Launch System acoustics: Far-field noise measurements of the Artemis-I launch," JASA Express Lett. **3**, 023601.

Gee, K. L., Mathews, L. T., Anderson, M. C., and Hart, G. W. (**2022**). "Saturn-V sound levels: A letter to the Redditor," J. Acoust. Soc. Am. **152**, 1068–1073.

Gee, K. L., Novakovich, D. J., Mathews, L. T., Anderson, M. C., and Rasband, R. D. (**2020**). "Development of a weather-robust ground-based system for sonic boom measurements," NASA/CR-2020-5001870, available at https://ntrs.nasa.gov/citations/20205001870 (Last viewed 14 November 2023).

GRAS (**2023**). "GRAS 46BE microphone specifications," available at https://www.grasacoustics.com/products/measurement-microphone-sets/constant-current-power-ccp/product/143-46be (Last viewed 14 November 2023).

Guest, S. H., and Jones, J. H. (**1967**). "Far-field acoustic environmental predictions for the launch of Saturn V and Saturn V MLV configuration," NASA TN D-4117, Washington, DC, available at https://ntrs.nasa.gov/citations/19670026446 (Last viewed 14 November 2023).
Hart, G. W., and Gee, K. L. (**2023**). "Correcting for ground reflections when measuring overall sound power level and acoustic radiation efficiency of rocket launches," Proc. Mtgs. Acoust. **50**, 040004.
Hart, G. W., Mathews, L. T., Anderson, M. C., Durrant, J. T., Bassett, M. S., Olausson, S. A., Houston, G., and Gee, K. L. (**2022**). "Methods and results of acoustical measurements made of a Delta IV Heavy launch," Proc. Mtgs. Acoust. **45**, 040003.
ISO (**2003**). 3745:2003, "*Acoustics—Determination of sound power levels of noise sources using sound pressure—Precision methods for anechoic and hemi-anechoic rooms*" (International Organization for Standardization, Geneva, Switzerland).
James, M. M., Salton, A. R., Gee, K. L., Neilsen, T. B., and McInerny, S. A. (**2014**). "Full-scale rocket motor acoustic tests and comparisons with empirical source models," Proc. Mtgs. Acoust. **18**, 040007.
Kellison, M. S., Gee, K. L., Cunningham, C. F., Coyle, W. L., Moore, T. M., and Hart, G. W. (**2023**). "Community-based noise measurements of the Artemis-I mission," Proc. Mtgs. Acoust. **51**, 040004.
Kenny, R. J., Hobbs, C., Plotkin, K. J., and Pilkey, D. (**2009**). "Measurement and characterization of Space Shuttle solid rocket motor plume acoustics," in *15th AIAA/CEAS Aeroacoustics Conference (30th AIAA Aeroacoustics Conference)*, 11–13 May, Miami, FL (American Institute of Aeronautics and Astronautics, Reston, VA), AIAA Paper 2009-3161.
Kramer, F. (**1966**). "Predicted acoustical performance of the S-1C sound suppressor," NASA TN D-3398, available at https://ntrs.nasa.gov/citations/19660014564 (Last viewed 14 November 2023).
Kumar, S. A., and Karthikeyan, N. (**2013**). "Prediction of launch vehicle noise during lift-off using a modified Eldred's method," in *The 14th Asia Congress of Fluid Mechanics –14ACFM*, October 15–19, 2013, Hanoi and Halong, Vietnam.
Leishman, T. W., Rollins, S., and Smith, H. M. (**2006**). "An experimental evaluation of the regular polyhedron loudspeakers as omnidirectional sources of sound," J. Acoust. Soc. Am. **120**, 1411–1422.
Lubert, C. P., Gee, K. L., and Tsutsumi, S. (**2022**). "Supersonic jet noise from launch vehicles: 50 years since NASA SP-8072," J. Acoust. Soc. Am. **151**, 752–791.
Marston, T. M. (**2008**). "Diffraction correction and low-frequency response extension for condenser microphones," M.S. thesis, Pennsylvania State University.
Mathews, L. T., Gee, K. L., and Hart, G. W. (**2021**). "Characterization of Falcon 9 launch vehicle noise from far-field measurements," J. Acoust. Soc. Am. **150**, 620–633.
Matoza, R. S., Fee, D., Neilsen, T. B., Gee, K. L., and Ogden, D. E. (**2013**). "Aeroacoustics of volcanic jets: Acoustic power estimation and jet velocity dependence," J. Geophys. Res. Solid Earth **118**, 6269–6284, https://doi.org/10.1002/2013JB010303.
Mayes, W. H. and Edge, P. M. (**1962**). "Noise measurements during captive and launch firings of a large rocket powered vehicle," NASA TN D-1502, available at https://ntrs.nasa.gov/citations/19630000776 (Last viewed 14 November 2023).
Mayes, W. H., Lanford, W. E., and Hubbard, H. H. (**1959**). "Near-field and far-field noise surveys of solid-fuel rocket engines for a range of nozzle exit pressures," NASA Report No. TN D-21, available at https://ntrs.nasa.gov/citations/19890068228 (Last viewed 14 November 2023).
McInerny, S. A. (**1992**). "Characteristics and predictions of far-field rocket noise," Noise Control Eng. J. **38**, 5–16.
Morshed, M. M. M., Hansen, C. H., and Zander, A. C. (**2013**). "Prediction of acoustic loads on a launch vehicle fairing during liftoff," J. Spacecr. Rockets **50**, 159–168.
NASA (**2022a**). See https://images-assets.nasa.gov/video/KSC-20221116-MH-AJN01-0001-Artemis_I_Isolated_Launch_Views-3314595/KSC-20221116-MH-AJN01-0001-Artemis_I_Isolated_Launch_Views-3314595~orig.mp4 (Last viewed 11 October 2023).
NASA (**2022b**). See https://images.nasa.gov/details/ART-CMA2_2022_320_0637_SHARED_art001m1203200637B (Last viewed 11 October 2023).
Potter, R. C. and Crocker, M. J. (**1966**). "Acoustic prediction methods for rocket engines, including the effects of clustered engines and deflected exhaust flow," NASA-CR-566, available at https://ntrs.nasa.gov/citations/19660030602 (Last viewed 14 November 2023).
Rasband, R. D., Gee, K. L., Gabrielson, T. B., and Loubeau, A. (**2023**). "Improving low-frequency response of sonic boom measurements through digital filtering," JASA Express Lett. **3**, 014802.
Smith, M., Craig, D., Herrmann, N., Mahoney, E., Krezel, J., McIntyre, N., and Goodliff, K. (**2020**). "The Artemis program: An overview of NASA's activities to return humans to the moon," in *2020 IEEE Aerospace Conference*, March 7–14, Big Sky, MT (Institute of Electrical and Electronics Engineers, Piscataway, NJ), pp. 1–10.
Varnier, J. (**2001**). "Experimental study and simulation of rocket engine free jet noise," AIAA J. **39**, 1851–1859.
Wilhold, G., Guest, S., and Jones, J. (**1963**). "A technique for predicting far-field acoustic environments due to a moving rocket sound source," NASA TN D-1832, Washington, DC.